Journal of Neonatal Surgery
ISSN(Online): 2226-0439
Vol. 14, Issue 32s (2025)
https://www.jneonatalsurg.com

OPEN ACCESS

Microwave Assisted Synthesis and Characterization of Titanium oxide, Thorium oxide and Mixed Metal Oxide Nanoparticles for anti bacterial Applications

Gomuraj Santhanaraj [1,2], Mathavan Alagarsamy [1]*

[1]Department of Chemistry, V.O.Chidambaram College, Tuticorin , Tamil nadu 628 008, India.

[2]Research scholar, Registration no. 17212232031002, Department of Chemistry, V.O.Chidambaram College, Tuticorin, Affiliated to Manonmaniam Sundranar university, Abishekapatti, Tirunelveli, Tamil nadu 627 012, India

Email.ID: abhimathavan@gmail.com

***Corresponding author:**

Dr. Alagarsamy Mathavan

Associate Professor and Head,PG & Research Department of Chemistry, V.O.Chidambaram College, Tuticorin – 628 008, Tamil nadu,India.

Email.ID: abhimathavan@gmail.com

Cite this paper as: Gomuraj Santhanaraj , Mathavan Alagarsamy , (2025) Microwave Assisted Synthesis and Characterization of Titanium oxide, Thorium oxide and Mixed Metal Oxide Nanoparticles for anti bacterial Applications. *Journal of Neonatal Surgery*, 14 (32s), 6426-6437.

ABSTRACT

Metal oxides demonstrate a range of unique properties, such as excellent chemical stability, versatile electrical conductivity, and catalytic abilities. In contrast, mixed metal oxides contain oxygen along with two or more distinct metallic elements. The presence of multiple metals gives mixed metal oxides innovative functionalities and properties that individual metal oxides lack. Titanium oxide and thorium(IV) oxide nanoparticles have attracted significant interest in various scientific and technological fields. This study explores a theoretical approach to synthesizing and characterizing metal oxides, specifically thorium(IV) oxide, titanium oxide, and TTMMO, a mixed metal oxide composed of titanium and thorium. The synthesis of nanoparticles is accomplished using the co-precipitation method with a A microwave reaction system was employed to synthesize nanoparticles, which were then characterized using various analytical techniques including FT-IR, UV-VIS (DRS), FE-SEM, EDAX, AFM, and XRD analysis. XRD analysis confirmed the cubic geometry of ThO_2 and the tetragonal structure of TiO_2 nanoparticles. Titanium oxide, thorium(IV) oxide, and titanium thorium mixed metal oxides (TTMMO) were evaluated for their antibacterial properties against E. Coli, Bacillus subtilis, Bacillus cereus, Pseudomonas aeruginosa, and Staphylococcus aureus using the disc diffusion technique. Extensive research has been conducted to investigate the exceptional antibacterial activities of these metal oxides and mixed metal oxides.

Keywords: *titanium oxide, thorium oxide, mixed metal oxides, E. Coli, and anti-bacterial studies*

1. INTRODUCTION

Nano particles possess distinct properties and behaviors that set them apart from larger counterparts, primarily due to their small size. This uniqueness makes them highly sought-after in a diverse range of applications. Because of their unique properties and wide-ranging applications, metal oxide nanoparticles have ushered in a new era of possibilities in the field of advanced materials [1]. Numerous studies has been conducted in recent years to investigate the potential of mixed metal oxides to create innovative materials by combining the desirable characteristics of various metal oxides [2]. Recent studies have reviewed a variety of techniques for making metal oxide and mixed oxide nanoparticles [3]. Among these methods, microwave-assisted co-precipitation method involves synthesizing nanoparticles by co-precipitating metal ions in the presence of microwave irradiation [4]. By utilizing microwave energy, the reaction kinetics are accelerated, leading to the rapid formation of nanoparticles. Surprisingly, the particle sizes, surface areas, and mechanical properties of the resulting materials can be altered by adjusting the temperature, operating conditions and precursor used [5]. In recent years, titanium oxide and thorium oxide have gained significant attention due to their exceptional properties and wide range of applications. These metal oxides have played a transformative role in various industries, thanks to their unique and advantageous characteristics. Moreover, the research on mixed metal oxides has paved the way for the development of advanced materials with enhanced performance. Understanding the properties and applications of titanium oxide, thorium oxide, and mixed

metal oxides allows us to leverage their potential and drive innovation in metal oxide technology.

Titanium dioxide, also referred to as titanium (IV) oxide or titania, is a versatile white pigment that is highly sought after and widely utilized across a range of industries. It is available in three primary crystalline forms rutile, anatase, and brookite, each offering unique characteristics that make titanium oxide a valuable material [5]. This compound demonstrates exceptional photocatalytic properties, a high refractive index, UV-visible absorption, and chemical stability, making it a preferred choice in numerous applications. It is commonly employed in the production of self-cleaning glass, air and water purification systems, and in the treatment of pollutants in wastewater. Titanium oxide is widely used in the cosmetics industry for its multifaceted applications. One important role it plays is as a key component in sunscreens, offering protection against harmful UV radiation by scattering and absorbing the rays. The distinctive optical characteristics of titanium oxide have also made it a valuable ingredient in pigments, particularly white paint and coatings [6].

Thoria, also known as thorium(IV) oxide, has garnered significant attention in recent years due to its unique properties. This compound possesses distinct characteristics that make it highly sought after for a variety of uses, including nuclear energy, catalysts, and electronic devices. The utilization of thorium(IV) oxide (ThO_2) as a sensing material in electronic devices has led to a breakthrough in technology known as thorium oxide sensing. Additionally, thorium oxide exhibits excellent electrical conductivity, making it well-suited for gas sensing applications [7]. With exceptional thermal stability, good electrical conductivity, and resistance to corrosion, thorium oxide is an ideal material for creating versatile and dependable sensors. The gas sensing technology of thorium oxide provides unmatched sensitivity, selectivity, and stability, making it a superior choice for various applications [8].

The objective of this study was to explore the potential of various metal oxides, including titanium oxide, thorium(IV) oxide, and a combination of titanium and thorium mixed metal oxides. The focus was on utilizing the microwave assisted co-precipitation method to synthesize and characterize these oxides, emphasizing their structural, electrical, and optical properties as well as topography. X-ray powder diffraction (XRD), field emission scanning electron microscopy (FE-SEM), FT-IR spectroscopy, UV-visible absorption spectroscopy, and atomic force microscopy were utilized for a comprehensive analysis of the nanoparticles. In recent times, there has been a surge in interest in the application of antibacterial studies across various industries such as environmental monitoring, manufacturing processes, and healthcare.

2.1. Materials and methods:

The metal oxides and mixed metal oxides were prepared using the microwave-assisted co-precipitation technique. All compounds utilized in this study were of analytical grade, including the precursors thorium nitrate ($Th(NO_3)_4$) and titanium oxy chloride sourced from Sigma Aldrich. The precipitant, sodium hydroxide (NaOH), was obtained from HiMedia. Double-distilled water was employed for the preparation of all solutions.

2.2. Instrumentation:

The FT-IR spectra ranging from 4000 to 400 cm-1 were recorded by utilizing KBR pellets and a Shimadzu 8400S spectrometer. XRD data was collected using a PANalytical X'pert-pro powder X'celerator diffractometer with Cu-kα radiation. UV-visible absorption and fluorescence spectra were examined with quartz cells using a JASCO FP-6300 spectrofluorometer and a JASCO variant-630 spectrophotometer. FE-SEM images were captured with a JEOL JSM-6700F field emission scanning electron microscope. The electrochemical studies were carried out by CH-Instrument Inc., a Texas-based company. AFM images were obtained with an Easy Scan 2 controller from Nanosurf, and contact mode measurements were conducted with a micromachined silicon probe.

2.3. Preparation of metal oxides and mixed metal oxides nanomaterials:

2.3.1. Preparation of Titanium dioxide (TiO_2)

The synthesis of Titanium dioxide (TiO_2) nanoparticles was carried out as follows: A 0.1M solution of titanium oxychloride ($TiOCl_2$) and a 0.3M solution of sodium hydroxide (NaOH) were prepared separately using double distilled water. The 0.3M NaOH solution was added dropwise to the 0.1M titanium oxychloride solution at a stirring rate of 500 rpm with a magnetic stirrer. The stirring rate was maintained at 500 rpm throughout the experiment by adjusting the revolution of the magnetic Teflon as the viscosity of the mixture increased. The addition of NaOH was continued until the desired pH was achieved. After completion of the addition, stirring was continued for approximately 2 hours to ensure homogeneity. A milky white suspension of $Ti(OH)_4$ was obtained during stirring. The solution was then irradiated with microwaves using a household microwave oven for 15 minutes at 150 W. The irradiated solution underwent sonication for 30 minutes at a frequency of 52 kHz to enhance the properties of the synthesized product. The resulting precipitate was filtered and washed with ethanol, followed by distilled water, before being dried in a hot air oven at 110°C for 2 hours. The dried powder was then annealed in a muffle furnace at 450°C for 3 hours to achieve pure white titanium dioxide.

2.3.2. Preparation of Thorium(IV) oxide (ThO_2) :

The standard procedure for synthesizing thorium(IV) oxide (ThO_2) nanoparticles involved preparing a 0.1M thorium nitrate solution in double distilled water and a separate solution of 0.3M sodium hydroxide (NaOH). The 0.3M NaOH solution was

then gradually added to the 0.1M thorium nitrate solution while stirring at 500 rpm with a magnetic stirrer. The addition process was halted once the desired pH level was achieved. Subsequently, the stirring continued for approximately 2 hours to ensure uniformity. The reaction between thorium nitrate solution and sodium hydroxide led to a hydrolysis reaction and the formation of products such as thorium hydroxide, resulting in the formation of a white colloidal dispersion. The solution is exposed to microwave irradiation for 15 minutes at 150 W in a microwave oven. Subsequently, the irradiated solution undergoes sonication for 30 minutes at a frequency of 52 kHz to enhance the properties of the resulting product. The resulting precipitate is isolated via filtration, undergoes washing with ethanol and distilled water, and is then dried in a hot air oven at 110°C for 2 hours. The dried powder is then annealed in a muffle furnace at 550°C for 2 hours to produce thorium(IV) oxide.

2.3.3. Synthesis of Titanium Thorium mixed metal oxide

The synthesis involved the use of titanium oxychloride ($TiOCl_2$) and thorium nitrate $Th(NO_3)_4$ as starting materials. Aqueous solutions of 0.1M $TiOCl_2$, 0.1M $Th(NO_3)_4$, and 0.3M NaOH were prepared separately using double distilled water. The NaOH solution was added dropwise to the $TiOCl_2$ solution, followed by the slow addition of the Th(NO3)4 solution. The mixture was stirred for 2 hours using a magnetic stirrer, then irradiated with microwaves for 15 minutes and sonicated at 52 kHz for 30 minutes to obtain the desired product. The resulting precipitate was collected, washed with ethanol and distilled water, and dried in a hot air oven at 110°C for 2 hours. The dried powder was then calcined in a muffle furnace at 550°C for 3 hours to produce the Titanium Thorium mixed metal oxide.

3. RESULTS AND DISCUSSION:

This study involved the synthesis of two metal oxide nanoparticles, specifically titanium oxide and thorium(IV) oxide, as well as a titanium thorium mixed metal oxide. Various analytical techniques were then employed to characterize these nanoparticles. UV-Visible absorbance (DRS) and FT-IR spectral methods were utilized to assess the optical properties of the nanoparticles. XRD analysis was conducted to investigate the crystal structure of the nanoparticles. Microstructural analysis, including size, shape, and composition, was carried out using Energy dispersive X-Ray (EDX) spectrometry and field emission scanning electron microscopy. Atomic force microscopy was used to study the topography images of the nanoparticles. The findings from these analyses are discussed in detail below.

3.1. Electronic spectra of nanomaterials (DRS):

The method of quantifying the light absorption of a sample within the UV and visible range is known as UV-Visible absorbance analysis, or Diffuse Reflectance Spectroscopy (DRS) [9]. It is a technique used to examine the absorbance and reflectance properties of solid materials across the visible and ultraviolet light spectrum [10]. Through the analysis of spectrum reflectance curves, UV-Visible DRS provides valuable insights into the chemical composition, structural features, and optical behavior of various solid samples.

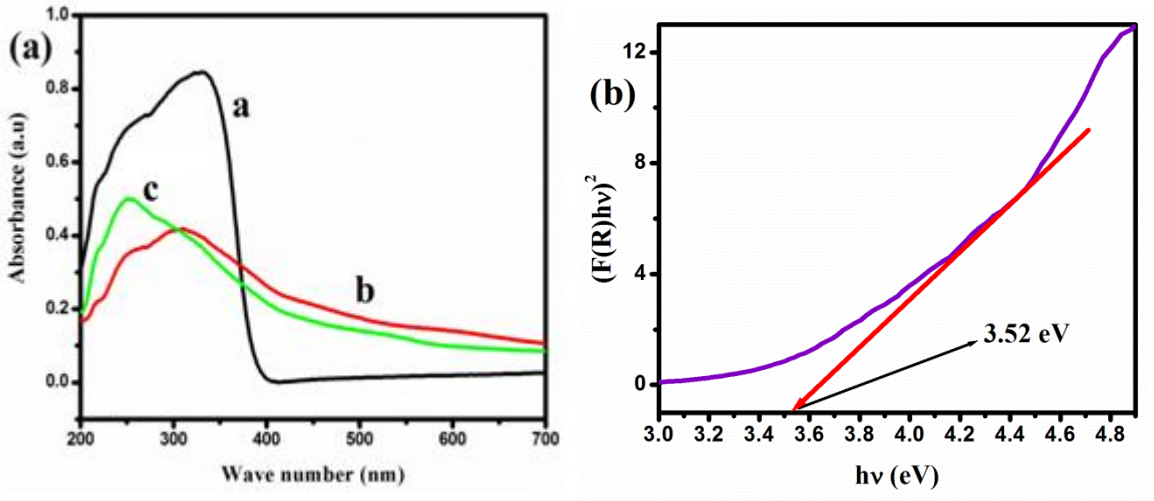

Figure.1. a) UV-Visible absorbance spectra of (a) TiO_2 (b) ThO_2 and (c) TTMMO

b) Kubelka-Munk plot of TTMMO

Utilizing UV-visible absorption spectroscopy, the optical characteristics of the nanoparticles prepared within the 200–700 nm wavelength range were investigated. As depicted in Fig. 1(a), titanium dioxide exhibited an absorbance value of 0.84 at 329 nm, indicating a strong absorption capacity in the UV region. The band gap energy of the TiO_2 nanoparticles was determined to be 3.77 eV. Similarly, thorium(IV) oxide displayed an absorption peak at 307 nm with a band gap energy of 4.04 eV, as shown in Fig. 1(b). Analysis of the spectra revealed a broad absorption peak at 250 nm for the mixed metal oxide,

suggesting significant absorbance in the visible region (A=0.90). This indicates a notable absorption capability in the visible range. The band gap energy of the mixed metal oxide was calculated to be 3.52 eV, with an absorption peak at 250 nm as illustrated in Fig.1(c). The Kubelka-Munk plot for the mixed metal oxide of titanium and thorium is illustrated in Figure 1 (b). The electronic properties of nanomaterials are tabulated in the Table.1.

Table.1. Absorption band (λ_{max}) and band gap energy values of Titanium oxide, Thorium oxide and TTMMO.

S.No	Name of the samples	Absorption band (λ_{max}) (nm)	Band gap energy (eV)
1	Titanium oxide	329	3.77
2	Thorium(IV) oxide	307	3.27
3	TTMMO	250	3.52

3.2. Fourier Transform – Infra Red Spectral Analysis:

FT-IR spectroscopy is a method used to examine how molecules interact with infrared radiation [11, 12]. The FT-IR spectra of titanium oxide, thorium oxide and mixed oxides of Ti and Th are given in Fig.2.

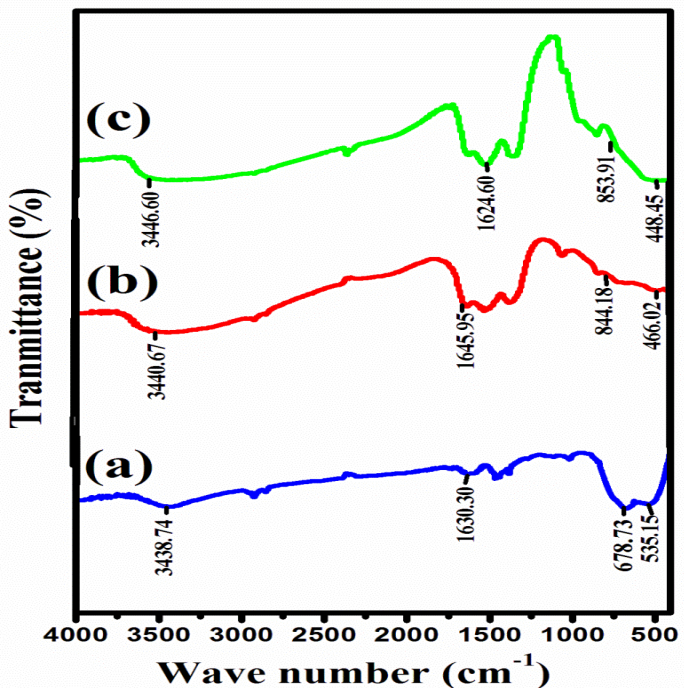

Figure.2. The FTIR spectrum of (a) Titanium oxide (b) Thorium oxide and (c) TTMMO

The infrared spectrum (FT-IR) of the synthesized TiO_2 reveals an absorption band at 3438.74 cm-1, indicating the stretching vibration of O-H and the presence of H_2O. Additionally, the bending vibration of O-H is observed at 1630.30 cm-1, while the intense peak at 678.73 cm-1 corresponds to the characteristic Ti-O stretching band associated with TiO_2. Similarly, the FT-IR spectrum of ThO_2 exhibits an absorption band at 3440.67 cm-1, indicating the stretching vibration of O-H and the presence of H_2O. The bending vibration of O-H is observed at 1645.95 cm-1, and intense peaks at 466.02 cm-1 and 844.18 cm-1 correspond to the characteristic Th-O stretching bands associated with ThO_2. The FT-IR spectrum of TTMMO shows an absorption band at 3446.60 cm-1, representing the stretching vibration of O-H and indicating the presence of H_2O (Fig.2). Similarly, the absorption band at 1624.60 cm-1 corresponds to the bending vibration of O-H. The strong peaks at 853.91 cm-1 and 448.45 cm-1 are indicative of the M-O stretching band specific to TTMMO, pointing towards the formation of a mixed metal oxide containing titanium (Ti-O) and thorium (Th-O). The FT-IR spectral data of various metal oxides are given in the Table.2.

Table.2. FT-IR spectral data for (1) Titanium oxide, (2) Thorium(IV) oxide and (3) TTMMO.

S.No	Name of the samples	Assigned functional groups		
		O-H Stretching vibration (cm^{-1})	O-H bending vibration (cm^{-1})	M-O stretching vibration (cm^{-1})
1	Titanium oxide	2307.58 3438.74	1384.19 1630.30	535.15 678.73
2	Thorium oxide	3440.67	1645.97	466.02 844.18
3	TTMMO	3446.60	1624.60	853.91 448.45

3.3. X Ray Diffraction Analysis:

X-ray diffraction analysis, also known as XRD analysis, is a non-destructive technique used to determine the arrangement of atoms or molecules within a crystalline material [13, 14].

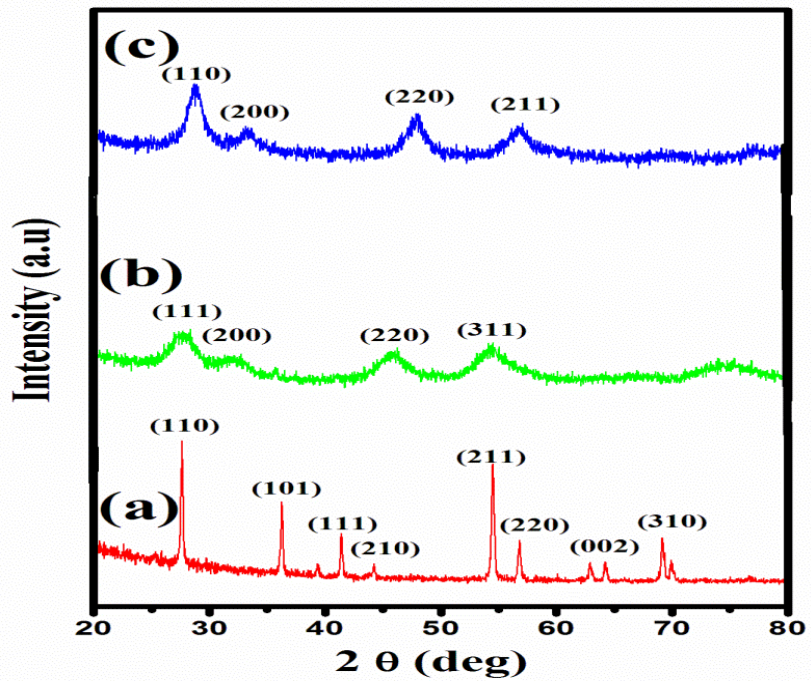

Figure.3. X-Ray Diffraction pattern of (a) Titanium oxide (b) Thorium oxide and (c) TTMMO

The titanium oxide samples in figure 3(b) exhibited characteristic peaks corresponding to various crystal planes, including (110), (101), (111), (210), (211), (220), (002), and (310). These findings aligned with the tetragonal structure identified in JCPDS file No. 89-4920 [15], providing further validation. By applying the Scherrer equation to analyze X-ray line broadening, the average size of the crystalline structures was estimated to be approximately 5.75 nm. The absence of peaks associated with other titanium oxide phases indicated a high level of purity in the prepared TiO_2 nanoparticles. The sharp, narrow peaks suggested the synthesized products were highly crystalline, underscoring the efficacy of the synthesis method utilized. The average crystallite size of the synthesized nanoparticles was determined using Scherrer's formula: $D = K\lambda/\beta\cos\theta$, where K represents the shape factor (typically 0.89), λ is the wavelength of the incident beam, β is the broadening of the diffraction line measured in radians at half of its maximum source (FWHM), θ is the Bragg's angle, and D is the diameter of the crystallite size. This calculation revealed that the average crystalline size of TiO_2 was approximately 5.75 nm. Additionally, the X-ray diffraction pattern of annealed ThO_2 nanoparticles indicated peaks at $2\theta = 27.64°$, 31.88°, 45.75°,

and 54.36°, corresponding to the (111), (200), (220), and (311) planes of crystalline ThO_2, respectively, in a cubic geometry (JCPDS file No. 4-0556) [16]. The XRD patterns of ThO_2 after annealing at 550 °C indicate a well-defined crystalline structure, showing reflections characteristic of cubic ThO_2 (see Fig. 3(b)). The calculated crystallite size for the material annealed at 550 °C is approximately 31.81 nm. The presence of diffraction peaks corresponding to mixed oxides at 2θ angles of 27.78°, 31.88°, 45.75°, and 54.33° suggests the presence of specific crystallographic planes within the TTMMO structure, such as (110), (200), (220), and (211) as depicted in Fig. 3 (c). An average crystallite size of 12.60 nm was determined based on the diffraction patterns observed. The interaction of Ti, O, and Th atoms within the lattice influences the growth and arrangement of the crystals, leading to a reduction in crystal size. This size reduction is attributed to limitations imposed on crystal growth by the presence of Ti-O-Th in the lattice structure. The crystallite size of the oxides are tabulated in the Table 3.

Table.3 Crystallite size of 1) Titanium oxide, 2) Thorium(IV) oxide and 3) TTMMO

S.No	Name of the samples	Crystallite Size (nm)
1	Titanium Oxide	5.75
2	Thorium(IV) Oxide	31.81
3	TTMMO	12.60

3.4. Energy-Dispersive X-Ray Analysis (EDAX) :

The Energy-Dispersive X-Ray Analysis (EDAX) technique is based on the X-ray fluorescence (XRF) principle. This method involves exposing a sample to high-energy X-rays, triggering the release of unique X-rays at varying energies from the atoms within the material. The Energy Dispersive X-ray Spectroscopy (EDS) was employed to analyze the elemental composition of metal oxides and mixed metal oxides [17]. Figure 4 represents the EDAX spectra of various prepared nanomaterials.

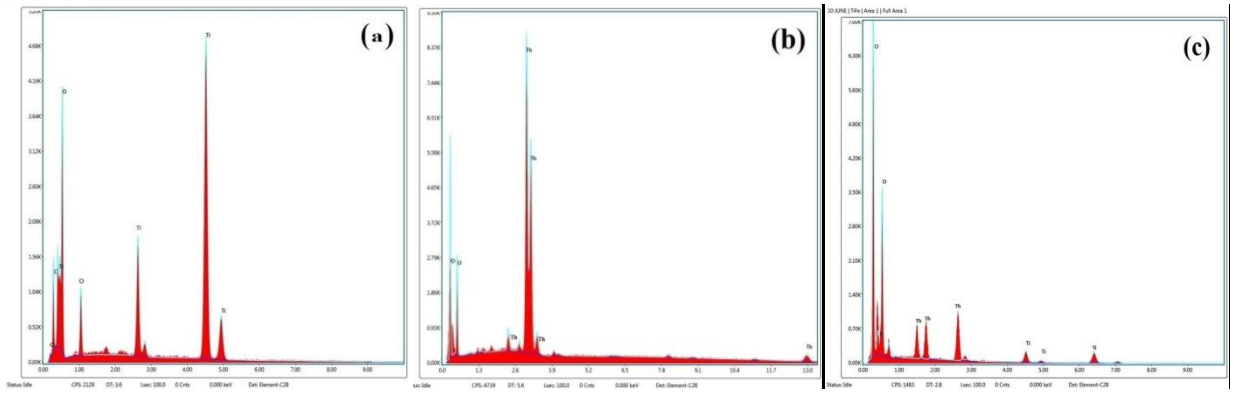

Figure.4. EDAX Spectral images of (a) Titanium oxide (b) Thorium(IV) oxide and (c) TTMMO

The EDS analysis of TiO_2 demonstrated the presence of titanium (Ti) and oxygen (O) in the material, as indicated by their respective weight percentages. The peaks observed in the EDS spectrum confirmed the existence of titanium and oxygen. Additionally, the analysis of the EDS spectrum confirmed that the titanium oxide nanoparticles obtained are highly pure, with the combined weight concentration of titanium and oxygen making up 100% of the total composition. Similarly, the EDS analysis of ThO_2 confirmed the existence of thorium (Th) and oxygen (O) in the material, as evidenced by their respective weight percentages. The elemental composition of ThO_2 was found to be oxygen (26.45%) and thorium (73.55%) by weight percentage. The peak at 2.8 keV indicated the presence of thorium, while the peak at 0.5 keV for oxygen clearly demonstrated the elemental composition and purity of ThO_2 nanoparticles. The examination of the EDS spectrum indicates that the thorium oxide nanoparticles acquired are of exceptional purity, with a total weight composition of 100.00%. The presence of titanium, thorium, and oxygen in both weight percent and atomic percent is definitively verified through the Energy Dispersive Spectroscopy (EDS) analysis of TTMMO. Specifically, the thorium peak at 2.8 keV, the titanium peak at 4.5 keV, and the oxygen peak at 0.5 keV depicted in [Fig. 4] elucidate the presence of these elements. This affirms the elemental constitution of the prepared TTMMO mixed metal oxides, wherein titanium comprises 34.80%, thorium 44.46%, and oxygen 20.74% of the elemental composition by weight percentage, summing up to 100.00%. The Elemental composition of titanium oxide, thorium oxide and TTMMO were shown in Table 4.

Table.4. Elemental composition of (a) Titanium oxide (b) Thorium(IV) oxide and (c) TTMMO.

Titanium oxide			b) Thorium(IV) oxide			c) TTMMO		
Element	**Weight %**	**Atomic %**	**Element**	**Weight %**	**Atomic %**	**Element**	**Weight %**	**Atomic %**
O K	52.77	75.93	**O K**	26.45	84.71	**O K**	20.74	41.08
Ti K	47.23	24.07	**Th M**	73.55	15.29	**Th K**	44.46	6.07
						Ti M	34.80	52.85
O K	100	100	**Total**	100	100	**Total**	100	100

3.5. FE-SEM analysis:

The Field Emission-Scanning Electron Microscopy (FE-SEM) is a high-resolution imaging technique that utilizes a focused beam of electrons to interact with the sample surface [18]. This beam scans the surface in a raster pattern, with the emitted secondary electrons creating a detailed image of the sample's topography. FE-SEM was employed to analyze the morphology and structure of the samples, providing clear, high to low magnification images down to the nanometer range [19]. The FE-SEM images of titanium oxide, thorium oxide, and TTMMO are shown in Figure 6.

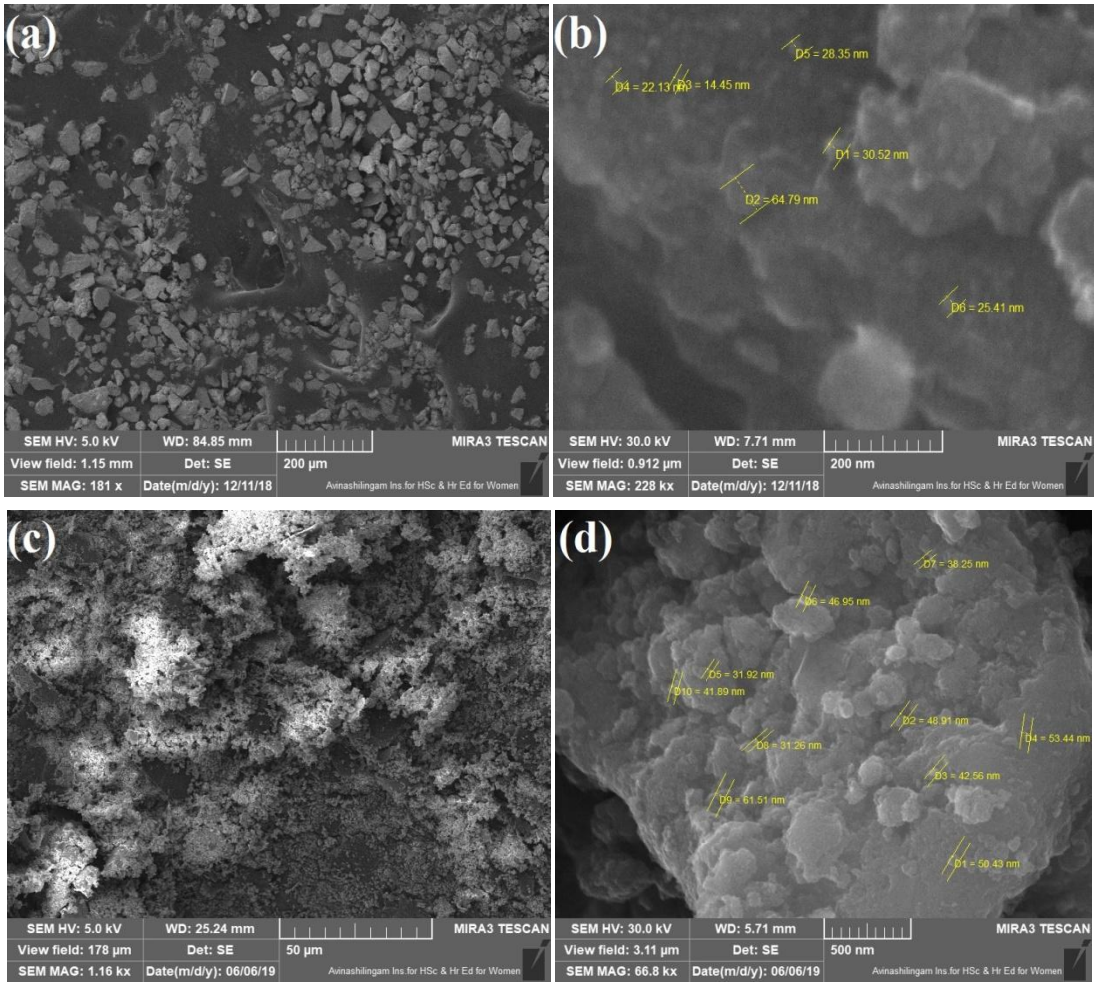

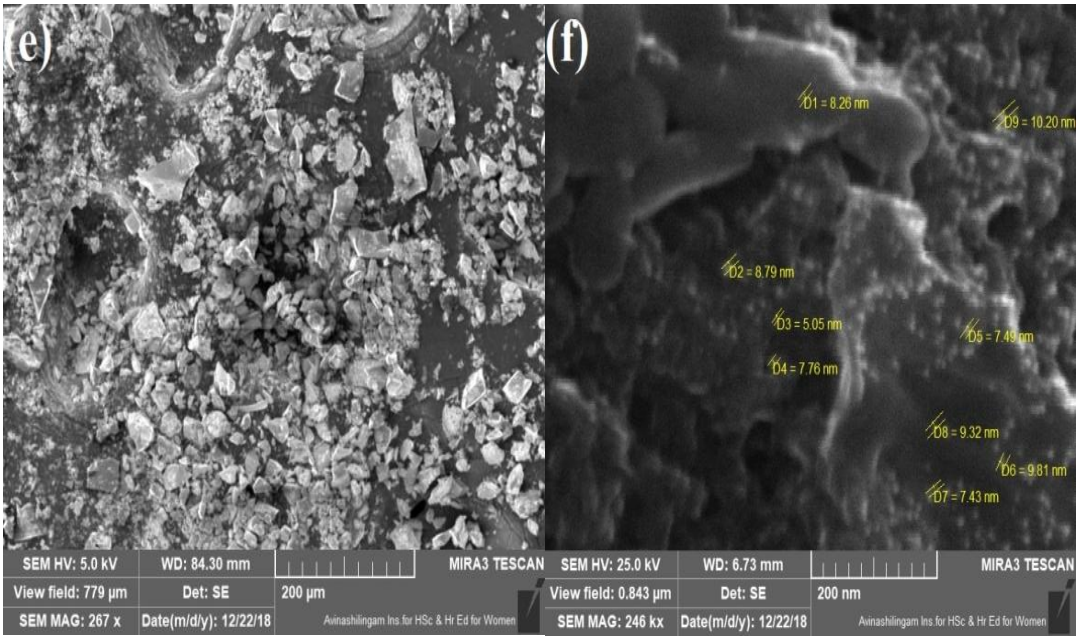

Figure.6. Shows the FE-SEM images of (a-b) Titanium oxide, (c-d) Thorium(IV) oxide and (e-f) TTMMO

The FE-SEM images of TiO_2 nanoparticles, synthesized using the microwave-assisted co-precipitation method, are depicted in Figure 6 (a-b). The sample, shown magnified by 200 µm, exhibits a granular structure with small spherical particles that are well-crystallized [40]. The average particle size of the TiO_2 nanoparticles, as estimated from the FE-SEM images, is approximately 31 nm (Figure 6(b)). These nanoparticles are evenly distributed and not agglomerated, indicating a high level of crystallinity induced by the annealing temperature [20]. The FE-SEM images of the annealed ThO_2 nanoparticles at 550 °C can be seen in Figure 6(c-d). The structure of the ThO_2 nanomaterial closely resembles a nanoreef when magnified by 50 µm. Moreover, the microscopic images revealed a consistent structure and even distribution of particles without any irregular surface formations. As seen in the FE-SEM images, the average particle size of ThO_2 is around 45 nm (Fig. 6(d)). The TTMMO, which was prepared, exhibited a nanofilm-like structure under a 200 µm magnification with an average particle size of 8 nm (Fig.6(f)). Comparatively, it is evident that the synthesized mixed metal oxide is smaller in size when compared to single oxides. This difference can be attributed to the higher annealing temperature and incorporation of mixed oxides in TTMMO, unlike single oxides.

3.6. Atomic Force Microscope spectral analysis:

Atomic Force Microscopy (AFM) is a crucial tool in the field of nanotechnology for both designing and characterizing nanoscale structures [21]. The AFM functions by utilizing a cantilever with a sharp tip to meticulously scan the surface of a sample at the atomic level. By measuring the forces between the tip and the sample, AFM is able to generate highly detailed three-dimensional images of nanoscale structures. Compared to optical microscopy, AFM provides superior resolution, making it an indispensable instrument for investigating phenomena at the nanoscale due to its ability to resolve characteristics down to the atomic level [22]. The morphology of prepared nanomaterials was examined using an atomic force microscope [23]. Each scan was conducted under ambient conditions to ensure satisfactory topography results. The images were captured in topography mode with a resolution of 256x256 pixels and a scan rate ranging from 0.5 to 1 Hz. Using the microscope's section analysis software, the heights of adsorbed NPs and agglomerates were measured [24]. The AFM spectral images of TiO_2, ThO_2, and mixed oxides of Ti and Th is shown in the Figure 7. As depicted in Figure 7, the AFM images of TiO_2 display a distinct grouping of conical nano columnar structures. Similarly, the AFM images of ThO_2 reveal a cluster of conical nanostructures. Notably, the TTMMO AFM images exhibit a mountain-like structure. These structures are further examined by the 3-D view of AFM which is shown in Fig.8.

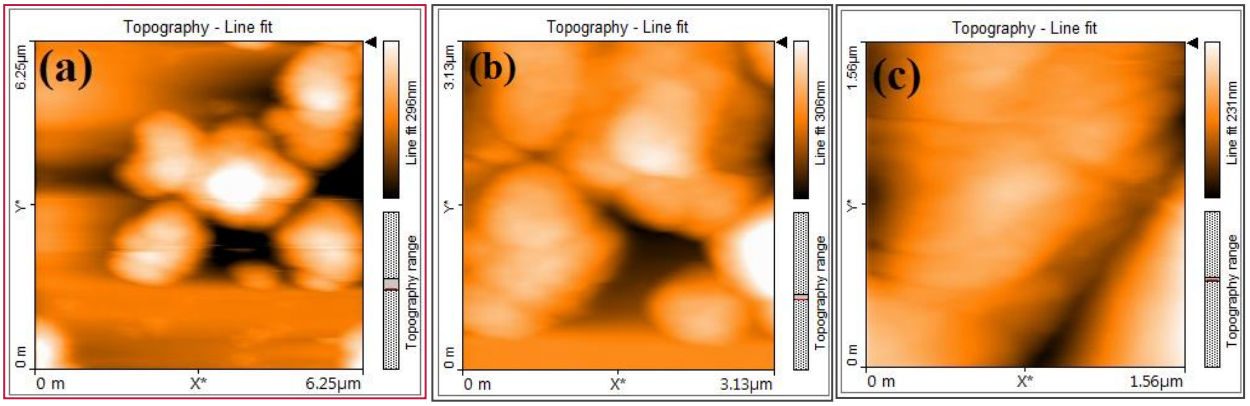

Figure.7. Atomic force microscope images of (a) Titanium oxide (b) ThO_2 and (c) TTMMO

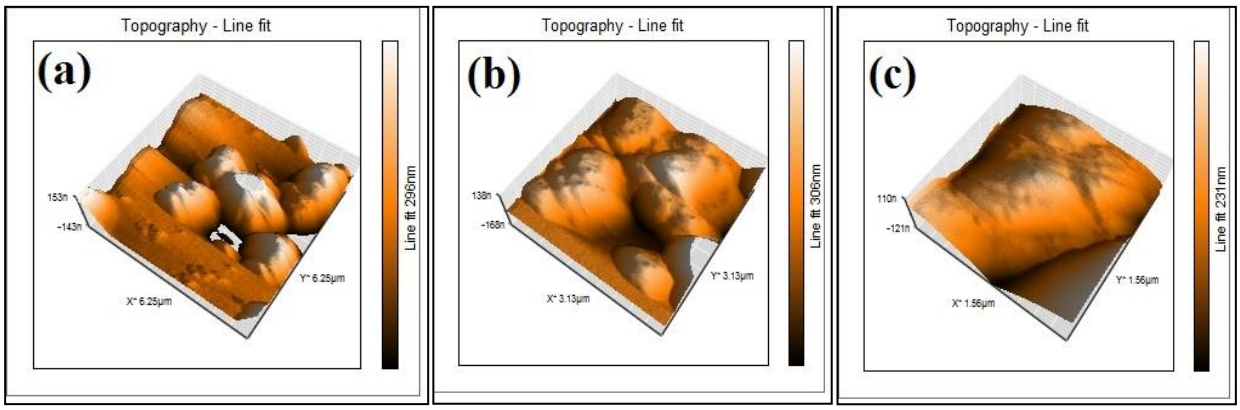

Figure.8. Atomic force microscope 3D view of (a) TiO_2 oxide (b) ThO_2 and (c) TTMMO

Upon analysis of the 3-D image, a mountainous structure resembling folds was observed in the prepared nanomaterials. Table 5 presents the commonly used area roughness parameters, including the average roughness (Sa) and root mean square roughness (Sq), which are measured across the entire three-dimensional surface. Specifically, the root mean square roughness (Sq) is utilized to examine spatial variations and temporal changes that occur during the formation of a new surface, allowing for analysis of surface features at different scales. It is essential to describe the surface topography using these roughness parameters.

Table.5. Area roughness of Titanium oxide, Thorium oxide and TTMMO from AFM spectroscopy

Area Roughness			
Area Parameter	**TiO_2**	**Thorium oxide**	**TTMMO**
Area	39.84 pm^2	39.84 pm^2	9.842 pm^2
S_a	42.27 nm	30.87 nm	5.81 nm
S_q	57.15 nm	38.23 nm	7.23 nm
S_y	409.13 nm	244.86 nm	44.09 nm
S_p	244.06 nm	126.49 nm	2.17 nm
S_v	-165.18 nm	-118.37 nm	-19.92 nm

S_m	-37.25 fm	-37.25 fm	-20.47 fm

4. Antibacterial activity of Titanium oxide, Thorium(IV) oxide and TTMMO :

Titanium oxide, thorium(IV) oxide, and TTMMO have gained significant attention in the field of antibacterial research due to their unique properties that make them highly effective against a broad spectrum of bacteria. These compounds show promising characteristics that offer a novel approach to antibacterial treatments. To investigate the antibacterial activity of titanium oxide, thorium(IV) oxide, and TTMMO against bacterial strains E. Coli, Bacillus subtilis, Bacillus cereus, Pseudomonas aeruginosa, and Staphylococcus aureus, the disc diffusion method was employed in this study. The test bacteria were first introduced into peptone water and allowed to incubate at 35ºC for 3 to 4 hours. Subsequently, sterile petri plates containing Mueller Hinton agar were prepared and poured with the bacterial suspension. A 0.1 ml volume of bacterial culture was applied onto the agar plates, then evenly spread using an L-rod. Subsequently, the inoculated plates were allowed to dry for five minutes before a disk containing a concentration of 1000 µg/ml of the test sample was gently placed on top of the petri plates with sterile techniques [25]. The plates were then incubated at 37ºC for 18 to 24 hours. Following incubation, the presence of a zone of inhibition was examined and measured in millimeters. Notably, all three nanoparticles demonstrated significant antibacterial properties, effectively inhibiting pathogen growth [26]. The largest zone of inhibition, measuring 12 mm, was observed for thorium oxide against Bacillus subtilis. The antibacterial activities of TiO_2, ThO_2 and TTMMO against Bacillus cereus are illustrated in Figure 9, while the levels of zone of inhibition are detailed in a table 6.

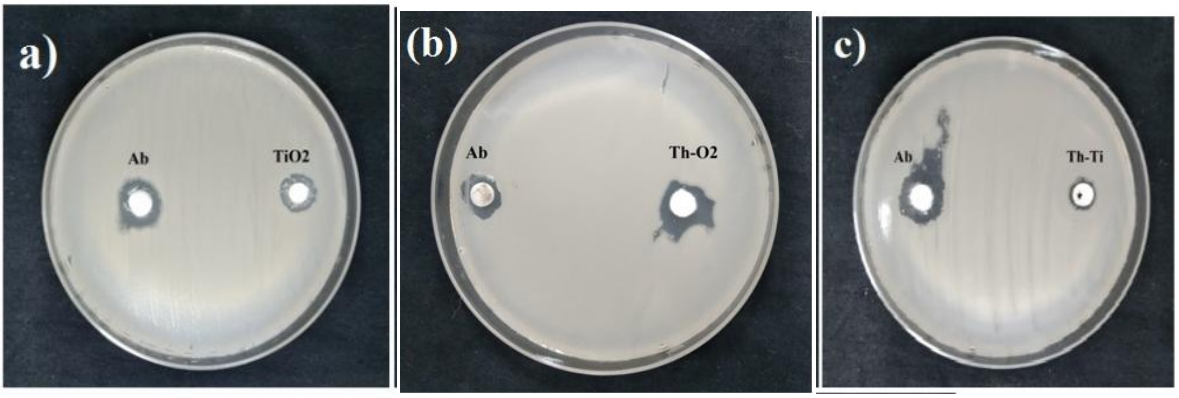

Figure.9. Antibacterial activity of (a) TiO_2 (b) ThO_2 and (c) TTMMO for *Bacillus cereus* bacterial strain

Table.6. Antibacterial activity Zone of inhibition levels for TiO_2, ThO_2 and TTMMO

Bacteria	Inhibition zone in mm					
	Ab Ampicillin	**TiO_2**	***Ab Ampicillin***	**ThO_2**	***Ab Ampicillin***	**TTMMO**
E.coli	7.5	8	10	9	11	9
Staphylococcus aureus	9	9	9	10	17	9
Bacillus subtilis	14	9	9	12	6	11
Bacillus cereus	7.5	6	10	7	8	8
Pseudomonas aeruginosa	8	8	10	9	14	10

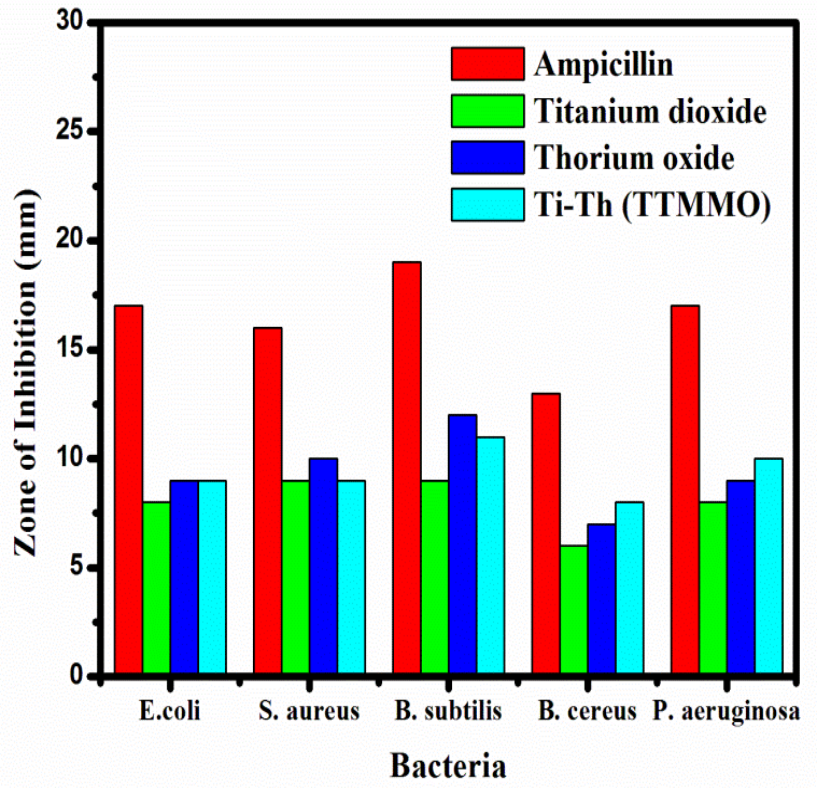

Figure.10. Antibacterial activity Zone of inhibition levels for TiO_2, ThO_2 and TTMMO

5. Conclusion:

The microwave-assisted co-precipitation method was employed to synthesize titanium oxide, thorium(IV) oxide, and mixed metal oxides of TTMMO with high purity, using the precursors of titanium oxy chloride and thorium nitrate. Various analytical techniques such as FT-IR, UV-VIS (DRS), XRD, FE-SEM, AFM, and EDAX were utilized for the characterization of the synthesized nanoparticles. The surface morphology of the metal oxide nanoparticles was examined through FE-SEM, revealing a diverse range of morphological structures. XRD analysis confirmed the nanocrystallite composition of the synthesized product, with the XRD pattern confirming the tetragonal structure of TiO_2 and the cubic structure of ThO_2. The high level of purity of the samples was validated by the EDAX results, disclosing their composition. The significant antibacterial activity of all three nanoparticles effectively hinders pathogen growth. The compounds demonstrated strong antimicrobial effects against E. coli, Bacillus subtilis, Bacillus cereus, Pseudomonas aeruginosa, and Staphylococcus aureus. Particularly, the use of thorium oxide against Bacillus subtilis resulted in the most substantial inhibition zone, measuring 12 mm. These findings suggest that these compounds could serve as promising alternatives to traditional antibacterial agents, offering an effective strategy to combat antibiotic resistance

REFERENCES

[1] M. Gouda, A. Aljaafari & W. E. Boraie, Preparation and characterization of some nanometal oxides using microwave technique and their application to cotton fabrics. Journal of Nanomaterials, (2015).https://doi.org/10.1155/2015/586904

[2] Damien Hudry, Christos Apostolidis & Daniel Meyer, Controlled synthesis of thorium and uranium oxide nanocrystals. Chemistry - A European Journal, (2013). https://doi.org/10.1002/chem.201203888

[3] Elisabetta Gabano & Mauro Ravera, Microwave-Assisted Synthesis: Can Transition Metal Complexes Take Advantage of This “Green” Method?. Molecules, (2022). https://doi.org/10.3390/ molecules27134249

[4] Qandeel Saleem, Milad Torabfam, Tuçe Fidan, Hasan Kurt, Meral Yüce, Nigel Clarke & Mustafa Kemal Bayazit, Microwave-Promoted Continuous Flow Systems in Nanoparticle Synthesis - A Perspective. ACS Sustainable Chemistry and Engineering, (2021).https://doi.org/10.1021/acssuschemeng.1c02695

[5] Imoisili, P. E., Jen, T. C., & Safaei, B. (2021). Microwave-assisted sol–gel synthesis of TiO2-mixed metal oxide nanocatalyst for degradation of organic pollutant. Nanotechnology Reviews, 10(1), 126-136.

[6] Schütz, M. B., Xiao, L., Lehnen, T., Fischer, T., & Mathur, S. (2018). Microwave-assisted synthesis of

nanocrystalline binary and ternary metal oxides. International Materials Reviews, 63(6), 341-374.

[7] O. N. Batuk, D. V. Szabo & S. N. Kalmykov, Synthesis and characterization of thorium, uranium and cerium oxide nanoparticles. Radiochimica Acta, (2013). https://doi.org/10.1524/ract.2012.2014

[8] Qiang Zhang, Zhenghua Qian & Yanbo Qiao, Synthesis of Thorium Dioxide Nanocrystals via Molten Salt Thermal Decomposition for Nuclear Energy-Related Applications. ACS Applied Nano Materials, (2022). https://doi.org/10.1021/acsanm.2c03961

[9] Brahma, S., Liu, C. P., & Shivashankar, S. A. (2017). Microwave irradiation assisted, one pot synthesis of simple and complex metal oxide nanoparticles: a general approach. Journal of Physics D: Applied Physics, 50(40), 40LT03.

[10] Benjaram M. Reddy, Pankaj Bharali & Tetsuhiko Kobayashi, Thermal stability and dispersion behavior of nanostructured Ce xZr1-xO2 mixed oxides over anatase-TiO2: A combined study of CO oxidation and characterization by XRD, XPS, TPR, HREM, and UV-Vis DRS. Industrial and Engineering Chemistry Research, (2009). https://doi.org/10.1021/ie8012677

[11] Divya Ananthanarayanan, Juan J. Diaz Leon, Jian Wei Ho, Mid-infrared characterization and modelling of transparent conductive oxides. Solar Energy, (2020). https://doi.org/10.1016/j.solener.2020.09.020

[12] Enrico Ridente, Mikhail Mamaikin & Nicholas Karpowicz, Electro-optic characterization of synthesized infrared-visible light fields. Nature Communications, (2022). https://doi.org/10.1038/s41467-022-28699-6

[13] Daniyal Kiani, X-Ray Diffraction (XRD). Springer Handbooks, (2023). https://doi.org/10.1007/978-3-031-07125-6_25

[14] Asif Ali, Yi Wai Chiang & Rafael M. Santos, X-Ray Diffraction Techniques for Mineral Characterization: A Review for Engineers of the Fundamentals, Applications, and Research Directions. Minerals, (2022). https://doi.org/10.3390/min12020205

[15] K, Sharmila, V.A, Kamat, K, Swaroop, H.M, Somashekarappa, AIP Conferenc Proceedings., 2019, October, (Vol. 2162, No. 1).

[16] Y. Huentupil, G. Cabello-Guzmán, B. Chornick, R. Arancibia & G.E. Buono-Core, Photochemical deposition, characterization and optical properties of thin films of ThO2. Polyhedron, (2018). https://doi.org/10.1016/j.poly.2018.10.023

[17] Bryan Shirley & Emilia Jarochowska, Chemical characterisation is rough: the impact of topography and measurement parameters on energy-dispersive X-ray spectroscopy in biominerals. Facies, (2022). https://doi.org/,10.1007/s10347-022-00645-4

[18] Ratnayake S, Lützenkirchen J & Finck N, Combined X-ray absorption and SEM–EDX spectroscopic analysis for the speciation of thorium in soil. Scientific Reports (2023). https://doi.org/10.1038/s41598-023-32718-x

[19] Pankaj B. Agarwal, Prathana Paulchowdhury & Navneet Kumar Thakur, Optimization of oxygen plasma based etching of single layered graphene through Raman and FESEM characterization. Materials Today: Proceedings, (2021). https://doi.org/10.1016/j.matpr.2021.05.587

[20] Anaya-Esparza, L. M., Montalvo-González, E., González-Silva, N., Méndez-Robles, M. D., Romero-Toledo, R., Yahia, E. M., & Pérez-Larios, A. (2019). Synthesis and characterization of TiO2-ZnO-MgO mixed oxide and their antibacterial activity. Materials, 12(5), 698.

[21] Thao Minh Ho, Felix Abik & Kirsi S. Mikkonen, An overview of nanoemulsion characterization via atomic force microscopy. Critical Reviews in Food Science and Nutrition, (2022). https://doi.org/10.1080/10408398.2021.1879727

[22] Li Mei & Guangzhao Guan, Profilometry and atomic force microscopy for surface characterization. Nano TransMed, (2023). https://doi.org/10.26599/ntm.2023.9130017

[23] David Alsteens, Hermann E. Gaub & Daniel J. Müller, Atomic force microscopy-based characterization and design of biointerfaces. Nature Reviews Materials, (2017). https://doi.org/10.1038/natrevmats.2017.8

[24] José Alvarez, Irène Ngo & Jean Pierre Simonato, Conductive-probe atomic force microscopy characterization of silicon nanowire. Nanoscale Research Letters, (2011). https://doi.org/10.1186/1556-276X-6-110

[25] Thakur, N., Thakur, N., Kumar, A., Thakur, V. K., Kalia, S., Arya, V & Kyzas, G. Z. (2024). A critical review on the recent trends of photocatalytic, antibacterial, antioxidant and nanohybrid applications of anatase and rutile TiO2 nanoparticles. Science of The Total Environment, 914, 169815.

[26] Akhtar, S., Shahzad, K., Mushtaq, S., Ali, I., Rafe, M. H., & Fazal-ul-Karim, S. M. (2019). Antibacterial and antiviral potential of colloidal Titanium dioxide (TiO2) nanoparticles suitable for biological applications. Materials Research Express, 6(10), 105409..